

Crystal Structure and Binding Properties of the CD2 and CD244 (2B4)-binding Protein, CD48^{*S}

Received for publication, February 10, 2006, and in revised form, May 1, 2006. Published, JBC Papers in Press, June 27, 2006, DOI 10.1074/jbc.M601314200

Edward J. Evans[‡], Mónica A. A. Castro^{S1}, Ronan O'Brien[¶], Alice Kearney^{||}, Heather Walsh[‡], Lisa M. Sparks[‡], Michael G. Tucknott^{||}, Elizabeth A. Davies^{||}, Alexandre M. Carmo^{S1}, P. Anton van der Merwe^{||2}, David I. Stuart^{**2}, E. Yvonne Jones^{**3}, John E. Ladbury[¶], Shinji Ikemizu^{††4}, and Simon J. Davis⁺⁵

From the [‡]Nuffield Department of Clinical Medicine, The University of Oxford and MRC Human Immunology Unit, Weatherall Institute of Molecular Medicine, John Radcliffe Hospital, Headington, Oxford OX3 9DS, United Kingdom, the ^SGroup of Cell Activation and Gene Expression, IBMC-Instituto de Biologia Molecular e Celular and ICBAS-Instituto de Ciências Biomédicas de Abel Salazar, Universidade do Porto, 4099-003 Porto, Portugal, the [¶]Department of Biochemistry and Molecular Biology, University College London, Gower Street, London WC1E 6BT, United Kingdom, the ^{||}Sir William Dunn School of Pathology, The University of Oxford, South Parks Road, Oxford OX1 3RE, United Kingdom, the ^{**}Division of Structural Biology, Wellcome Trust Centre for Human Genetics, The University of Oxford, Roosevelt Drive, Oxford OX3 7BN, United Kingdom, and the ^{††}Division of Structural Biology, Graduate School of Pharmaceutical Sciences, Kumamoto University, 5-1 Oe-honmachi, Kumamoto 862-0973, Japan

The structural analysis of surface proteins belonging to the CD2 subset of the immunoglobulin superfamily has yielded important insights into transient cellular interactions. In mice and rats, CD2 and CD244 (2B4), which are expressed predominantly on T cells and natural killer cells, respectively, bind the same, broadly expressed ligand, CD48. Structures of CD2 and CD244 have been solved previously, and we now present the structure of the receptor-binding domain of rat CD48. The receptor-binding surface of CD48 is unusually flat, as in the case of rat CD2, and shares a high degree of electrostatic complementarity with the equivalent surface of CD2. The relatively simple arrangement of charged residues and this flat topology explain why CD48 cross-reacts with CD2 and CD244 and, in rats, with the CD244-related protein, 2B4R. Comparisons of modeled complexes of CD2 and CD48 with the complex of human CD2 and CD58 are suggestive of there being substantial plasticity in the topology of ligand binding by CD2. Thermodynamic analysis of the native CD48-CD2 interaction indicates that binding is driven by equivalent, weak enthalpic and entropic effects, in contrast to the human CD2-CD58 interaction, for which there is a large entropic barrier. Overall, the structural and biophysical comparisons of the CD2 homologues suggest that the evolutionary diversification of interacting cell surface proteins is rapid and constrained only by the requirement that binding remains weak and specific.

The CD2 subset of the immunoglobulin superfamily (IgSF)⁶ consists of generally small hematopoietic cell-cell recognition proteins encoded by two groups of genes located on either side of the centromere of human chromosome 1. Genes on the *p* arm encode the prototypical proteins, CD2 and CD58 (also known as LFA-3), whereas the *q* arm genes encode the set of nine proteins known collectively as the "SLAM family," *i.e.* BLAME, SF2001 (CD2F10), NTBA (SF2000), CD84, CD150 (SLAM), CD48, CS1 (19A, CRACC), CD229 (Ly9), and CD244 (2B4) (reviewed by Engel *et al.* (1)). Six members of the SLAM family carry the tyrosine phosphorylation motif, Thr-Ile/Val-Tyr-Xaa-Xaa-Val/Ile, which binds a protein consisting of a single Src homology domain. This protein is known as SLAM-associated protein, or SAP, and it is encoded by the gene whose mutation leads to X-linked lymphoproliferative disease (2). The expression of combinations of SLAM family proteins, *i.e.* SLAM, CD48, and CD244, differentiate hematopoietic stem cells and progenitors, but the physiological significance of this is unclear given, *e.g.*, that SLAM-deficient mice have normal numbers of stem cells (3).

Work on CD2-deficient mice has shown that the CD2-CD48 interaction is not essential for the development or function of an apparently normal immune system (4). Instead, CD2 has a more subtle role in setting TCR-affinity thresholds for T-cell activation, thereby "fine-tuning" the T-cell repertoire (5–8). Mice deficient in CD48, which is expressed on most hematopoietic cells, on the other hand, exhibit a more severe phenotype in which the activation of CD4⁺ T cells is severely impaired (9), suggesting that CD48 is not restricted to interactions with CD2. Consistent with this possibility, CD48 is now known to bind CD244 in mice and humans (10). CD244 is expressed on NK cells, and a subset of T cells and is involved in triggering the non-major histocompatibility complex-restricted killing of CD48-expressing target cells (11–13). Two rat homologues of CD244 have been identified (14, 15), and the

^{*} The costs of publication of this article were defrayed in part by the payment of page charges. This article must therefore be hereby marked "advertisement" in accordance with 18 U.S.C. Section 1734 solely to indicate this fact.

^S The on-line version of this article (available at <http://www.jbc.org>) contains supplemental Figs. S1–S3.

¹ Supported by the Programa Operacional Ciência e Inovação 2010 (POCI), co-funded by the European Regional Development Fund (FEDER).

² Supported by the UK Medical Research Council.

³ Supported by Cancer Research UK.

⁴ Supported by Grants-in-Aid from the Ministry of Education, Culture, Sports, Science and Technology of Japan. To whom correspondence may be addressed: Tel./Fax: 81-96-371-4647; E-mail: ikemizu@gpo.kumamoto-u.ac.jp.

⁵ Supported by the Wellcome Trust. To whom correspondence may be addressed: Tel: 44-1865-221-336; Fax: 44-1865-222-737; E-mail: simon.davis@ndm.ox.ac.uk.

⁶ The abbreviations used are: IgSF, immunoglobulin superfamily; s, soluble; r, rat; h, human; m, mouse; c, chimeric; WT, wild-type; PDB, Protein Data Bank; r.m.s.d., root mean square deviation; NK, natural killer cells; TCR, T-cell receptor.

structure of the mouse homologue has been determined using NMR methods (16). Apart from the interaction of human CD2 with CD58 (17), of murine CD48 with CD2 (18) and CD244 (10), and of human SLAM with itself (19), the network of interactions of the CD2 subset of the IgSF is uncharacterized; there is some evidence, however, that, like SLAM, several of the proteins are homophilic (reviewed by Engels *et al.* (1)).

The interactions of CD2 with its ligands, such as CD48, have provided important insights into the nature of weak, specific recognition at the cell surface (20). The low affinity of such interactions allows multivalent contacts between cells expressing these molecules to be transient (21). The ligand affinities of most leukocyte surface proteins are more than four orders of magnitude weaker than, *e.g.* antibody-antigen interactions ($K_d \sim 1$ nM), with their K_d values clustering in the region of 5–20 μ M. The interaction of rat CD2 with CD48 is unusual in that it lies well outside this range (65 μ M; reviewed in Refs. 22 and 23). Structural (24, 25) and mutational (26) studies suggest a binding mechanism that ensures such weak interactions are nevertheless specific. Mutations of more than half of the charged residues clustered in the ligand binding face of CD2 compromise the specificity rather than the strength of its binding to CD48 (26). This effect likely results from the requirement that electrostatic complementarity compensates for the removal, upon binding, of water interacting with the charged residues. This mode of recognition is well suited to interactions requiring a low affinity, because it uncouples increases in specificity from increases in affinity.

Support for such a proposal emerged from structural analyses of human CD2 (25) and both crystallographic (27) and NMR-based (28) analyses of CD58, which revealed a high degree of electrostatic complementarity of the respective binding surfaces. The possibility that specificity depends largely on electrostatic complementarity was confirmed by the prediction of the topology of the CD2-CD58 complex prior to publication of the actual complex (29), based on maximizing the degree of electrostatic complementarity in a model of the complex (27). An additional, important property of the interaction revealed by the complex structure is the lack of surface complementarity between the ligand binding faces of CD2 and CD58 (29), which stands in marked contrast to the interfaces of proteins that interact in solution (30).

CD48 is necessary for both cognate recognition, *i.e.* by T cells (in rats and mice), and non-antigen-specific lymphocyte activation, *i.e.* by NK cells (in all species studied). The crystal structure of the ligand-binding domain of rat CD48, presented here, completes the initial structural characterization of the murine CD2/CD244/CD48 receptor-ligand system and allows the generality of observations based on analysis of the human CD2-CD58 complex to be tested for a second weakly interacting receptor-ligand pair. Although the new structural data lend considerable support to the idea that the specificity of interactions within the CD2 subset is highly dependent on electrostatic contacts, a thermodynamic analysis reveals unexpected differences in the mechanism of ligand binding by rat CD2 *versus* that by the human protein (human interaction character-

ized by Kearney *et al.*⁷). Overall, our observations suggest that the evolutionary diversification of interacting cell surface proteins is rapid and constrained only by the requirement that binding is weak and specific.

EXPERIMENTAL PROCEDURES

Protein Production—Briefly, for chimeric (c) CD48, *in vitro* mutagenesis was used to replace the sequence encoding the C2-set domain of the extracellular region of rat CD48 with the analogous rat CD2 domain. The mature cCD48 polypeptide started with the native CD48 N-terminal sequence “FQDQ . . .,” continued to the CD48 domain 1/CD2 domain 2 junctional sequence “ . . . MEVY/EMVS . . .,” and ended with the C-terminal sequence “ . . . CPEK” of domain 2 of rat CD2. The construct was expressed in Lec3.2.8.1 cells using the glutamine synthetase-based gene expression system in the presence of 0.5 mM *N*-butyldeoxynojirimycin (a kind gift of R. A. Dwek of the Glycobiology Institute, Oxford) as described previously (31). Protein was purified by affinity chromatography using the OX45 antibody and gel filtration, deglycosylated using endoglycosylase H at pH 5.2 and 37 °C for 90 min, and re-purified by gel filtration. Soluble forms of rat CD2 and CD48 (srCD2 and srCD48) were produced by similar methods, as described before (24). The wild type (WT) and mutant R87A forms of domain 1 of rat CD2 were expressed in the form of fusion proteins with glutathione *S*-transferase in *Escherichia coli*, which were cleaved with thrombin so that the monomeric CD48-binding domain of CD2 could be isolated, as described (32). WT and mutant forms of rat CD48 used for binding studies were expressed as chimeras of the extracellular region of CD48 fused to domains 3 and 4 of rat CD4 and a BirA recognition tag, as described (33), by transient transfection of 293T cells in X-VIVO 10 serum free medium (BioWhittaker). Mutants were generated directly in the expression vector (pEF-BOS (34)) either by using the Muta-Gene Phagemid Mutagenesis Kit version 2 (Bio-Rad) or by PCR with mutagenic oligonucleotide primers. All mutations were confirmed by complete sequencing of the vector constructs.

Crystallization, Structure Determination, and Analysis of cCD48—Deglycosylated, purified cCD48 at a concentration of 15 mg/ml was crystallized by sitting drop vapor diffusion (35) in the presence of 1.5 M lithium sulfate, buffered at pH 7.5 with 0.1 M sodium HEPES (Crystal Screen solution from Hampton Research, Riverside, CA). Crystals were briefly transferred to a freezing solution made by adding glycerol to the precipitant solution to a final concentration of 30% before being cooled to 100 K for data collection. Diffraction data were collected on beamline ID2 at the European Synchrotron Radiation Facility (Grenoble, France) using a 34.5-cm MAR-Research (Hamburg, Germany) image plate detector. Data were processed and scaled using Denzo and Scalepack (36). Phases were determined by molecular replacement using AmoRe (37) and the coordinates of domain 2 of rat CD2 (24), which gave an unambiguous solution for the position of domain 2. A model, using the coordinates of cCD58 (27) with the residues in domain 1

⁷ A. Kearney, A. Avramovic, M. A. A. Castro, A. M. Carmo, S. J. Davis, and P. A. van der Merwe, unpublished data.

substituted with polyalanine, was positioned on this solution. After two-domain rigid body refinement in CNS (38), this model gave an R -factor of 46.7%. Solvent flattening was performed using DM (39), and refinement was carried out using CNS (38), with manual rebuilding in O (40). After simulated annealing, positional refinement and overall B -factor refinement in CNS, $2F_o - F_c$ and $F_o - F_c$ electron density maps showed bias-free density, and the correct sequence could be substituted into domain 1. Further positional and individual B -factor refinement was then carried out, with bulk solvent correction, using all the observed data but with 5% of the data set aside for R_{free} cross-validation in 24 refinement cycles.

Structural superpositions were performed using SHP (41). Figs. 1, 2, and 5 were produced using Bobscript (42), Raster 3D (43), and Volumes.⁸ GRASP (44) was used for the electrostatic analysis and surface display in Figs. 3 and 4. The improved model for the complex between rat CD2 and CD48 was initially generated by superposition of these molecules on the human CD2-CD58 complex (PDB id 1qa9 (29)), followed by manual adjustment to align the residues known to interact by mutagenesis (see text). This model was then refined using MultiDock (45), and atoms within 4 Å, allowing for side-chain rotamer combinations that did not result in steric clashes between the proteins, were identified as possible contacts.

Isothermal Titration Calorimetry—All experiments were performed using the MCS system (Micro Cal, LLC, Northampton, MA) as described (46, 47). In a typical experiment, 1.75 mM srCD48 was added in twenty 12-μl injections to a 0.09 mM solution of the WT or mutant rCD2 V-set IgSF domain in the 1.3-ml calorimeter cell at the temperature indicated. Ionic strength was varied by diluting the proteins into buffers containing the indicated NaCl molarities prior to the experiments. The resulting data were fitted as described (46) after subtracting the heats of dilution, resulting from addition of sCD2d1 to buffer and buffer to srCD48, determined in separate control experiments. Titration data were fitted using a non-linear least-squares curve-fitting algorithm with three floating variables: stoichiometry, association constant (K_a), and change of enthalpy on binding (ΔH_{obs}). Isothermal titration calorimetry gives a complete thermodynamic characterization of an interaction based on Equation 1,

$$\Delta G = -RT \times \ln(K_a) = \Delta H_{\text{obs}} - T\Delta S \quad (\text{Eq. 1})$$

where R is the gas constant, T is the absolute temperature, and ΔG , ΔH_{obs} , and ΔS are the standard free energy, enthalpy, and entropy changes on going from unbound to bound states, respectively. All experiments were done in triplicate.

Binding Studies—Binding experiments were performed on BIAcore 2000 or BIAcore 3000 instruments (Biacore AB, Uppsala, Sweden) at 25 °C in the running buffer HBS-EP (10 mM HEPES, pH 7.4, 150 mM NaCl, 3 mM EDTA, 0.005% surfactant P20). For analysis of CD2 binding by cCD48, OX54 was coupled covalently to a CM5 research grade sensor chip (Biacore AB) via primary amines using the standard amine coupling kit (Biacore

AB). OX54 was injected at 100 μg/ml in 10 mM sodium acetate (pH 5) giving immobilization levels of 6,000–8,000 response units. For analysis of CD2 binding by WT and mutant CD48, the binding of srCD2 to biotinylated CD48-CD4 chimeras was analyzed. Streptavidin was immobilized on a CM5 chip by amine coupling as above. Streptavidin was injected at 0.5 mg/ml in 10 mM sodium acetate (pH 5.5) and immobilized to a level of 9,000–10,000 response units. Supernatant from 293T cells transiently transfected with the CD48-CD4 chimeric constructs was concentrated and exchanged into 10 mM Tris-HCl (pH 8) for biotinylation with the enzyme BirA (Avidity, Denver, CO). Biotinylated supernatant was injected until immobilization levels of ~2,000 response units were obtained. To calculate dissociation constants, equilibrium binding was measured after injection of rCD2d1 (if immobilization was via OX54) or srCD2 at various concentrations. Specific binding was calculated by subtracting the response in a control flow cell containing only immobilized OX54 or biotinylated rat CD4 domains 3 and 4 immobilized via streptavidin. Binding data were fitted with a 1:1 Langmuir binding model to calculate K_d . For van't Hoff analysis, the K_d for the interaction of srCD2 with immobilized WT CD48-CD4 chimera was calculated from affinity data obtained at several different temperatures. ΔG values were calculated using Equation 1 and plotted against temperature. These data were fitted with the non-linear van't Hoff equation (48) to estimate values for ΔH_{vH} , ΔS_{vH} , and $\Delta C_{p, \text{vH}}$ at 25 °C or 37 °C (Equation 2),

$$\Delta G = \Delta H_{\text{vH}, T_0} - T\Delta S_{\text{vH}, T_0} + \Delta C_{p, \text{vH}}(T - T_0) - T\Delta C_{p, \text{vH}} \ln(T/T_0) \quad (\text{Eq. 2})$$

where T is the temperature in Kelvin (K); T_0 is an arbitrary reference temperature (e.g. 298.15 K for calculation of constants at 25 °C); ΔG is the standard free energy of binding at T (kcal mol⁻¹); $\Delta H_{\text{vH}, T_0}$ and $\Delta S_{\text{vH}, T_0}$ are the enthalpy and entropy changes upon binding at T_0 (kcal mol⁻¹ and kcal mol⁻¹K⁻¹, respectively); and $\Delta C_{p, \text{vH}}$ is the change in heat capacity (kcal mol⁻¹K⁻¹, assumed to be temperature-independent). Theoretical calculation of ΔC_p based on measurement of the solvent-accessible surface area buried on binding utilized the relationship of Spolar *et al.* (49).

RESULTS

Expression of a Crystallizable Form of Rat CD48—A soluble form of rat CD48 (srCD48), consisting of the entire extracellular region of the protein was expressed in Lec3.2.8.1 CHO cells, yielding protein with endoglycosidase H-sensitive N -glycosylation (50). Deglycosylated srCD48 did not crystallize alone, and although it crystallized in a complex with the rat CD2 extracellular domain (srCD2, data not shown), these crystals did not diffract. In an alternative strategy, a chimeric form of the protein (cCD48) consisting of the CD48 ligand-binding, V-set IgSF domain and the membrane-proximal, C2-set IgSF domain of rat CD2 was generated, because this approach had been successful with human CD58 (27). cCD48 was expressed in Lec3.2.8.1 cells in the presence of N -butyldeoxynojirimycin (31). The deglycosylated form of this protein bound srCD2 with WT affinity (supplemental Fig. S1), indicating that it is correctly

⁸ R. Esnouf, personal communication.

TABLE 1

Data collection and refinement statistics for the cCD48 structure

| | |
|---|------------------------|
| Data collection statistics | |
| Wavelength (Å) | 0.977 |
| Resolution limits (Å) | 30–2.6 |
| Space group | 14 ₁ 22 |
| Unit cell dimensions (Å) | 96.78 × 96.78 × 126.62 |
| Number of observations | 112,655 |
| Unique reflections ^a | 9,426 (623) |
| Completeness (%) ^a | 98.5 (99.4) |
| <i>I</i> /σ(<i>I</i>) ^a | 25.1 (2.9) |
| <i>R</i> _{merge} (%) ^{a,b} | 6.3 (61.0) |
| Structure refinement statistics | |
| Resolution limits (Å) | 30–2.6 |
| Reflections (<i>F</i> > 0) | 9,400 |
| Completeness (%) | 98.2 |
| Reflections in (5%) test set | 501 |
| <i>R</i> _{cryst} (%) ^{a,c} | 21.6 (40.7) |
| <i>R</i> _{free} (%) ^{a,c,d} | 27.2 (47.1) |
| Number of non-hydrogen atoms | 1,596 |
| Protein | 1,481 |
| Sugar | 43 |
| H ₂ O | 42 |
| Glycerol | 30 |
| Geometry r.m.s.d. | |
| Bond lengths (Å) | 0.010 |
| Bond angles (°) | 1.6 |
| Average <i>B</i> factors (Å ²) | |
| Protein | 56.4 |
| Sugar | 77.9 |
| Water | 49.0 |
| Glycerol | 67.6 |
| Main chain | 54.3 |
| Side chain | 58.3 |
| <i>B</i> factor r.m.s.d. (Å ²) | |
| Main chain bonds | 2.6 |
| Side chain bonds | 4.1 |
| Main chain angles | 4.3 |
| Side chain angles | 6.1 |

^a Numbers in parentheses refer to highest resolution shell (2.66–2.60 Å for data processing and 2.69–2.60 Å for structure refinement).

^b $R_{\text{merge}} = \sum |I_j - \langle I \rangle| / \sum I_j$, where I_j is the intensity of an individual observation of a reflection and $\langle I \rangle$ is the average intensity of that reflection.

^c $R_{\text{cryst}} = \sum ||F_o| - |F_c|| / \sum |F_o|$, where $|F_o|$ is the observed structure factor amplitude and $|F_c|$ is the calculated structure factor amplitude.

^d R_{free} is calculated as for R_{cryst} but only against the test data excluded from refinement.

folded and functional. Small crystals of cCD48 were obtained by using the sitting drop vapor diffusion method. After growth for up to 12 months, the crystals reached a size sufficient for diffraction analysis using a microfocus beamline.

Structure Determination and Overall Structure of cCD48—X-ray diffraction data to 2.6-Å resolution were collected, and the structure was solved by molecular replacement with the coordinates of the C2-set membrane-proximal IgSF domain of rat CD2, followed by modeling of the V-set ligand-binding domain of CD48 based on the peptide backbone of the equivalent domain from human CD58. After final refinement, the structure had an *R*-factor of 21.6% and a free *R*-factor of 27.2%; additional measures of data and refinement quality are given in Table 1. Three residues in the final structure (Gln-4, Pro-25, and Thr-37) have phi-psi angles that fall outside the allowed regions of the Ramachandran plot. Two of these are in the poorly ordered N terminus and BC loop of the V-set IgSF domain (Gln-4 and Pro-25). The third (Thr-37) is part of an unusual loop structure that can be manually fitted to the electron density but does not refine well. The structure of this loop and the surrounding electron density are shown in supplemental Fig. S2. Electron density was observed at all three potential glycosylation sites, allowing modeling of the GlcNAc residues (e.g. supplemental Fig. S2). The final model includes 42 water

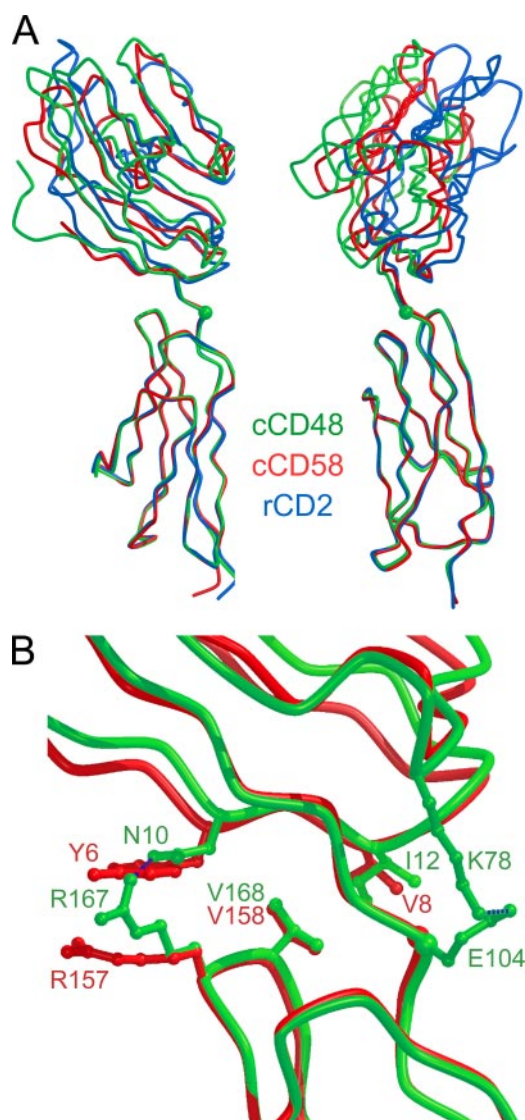


FIGURE 1. The structure of cCD48. A, two orthogonal views of schematic α -carbon representations of cCD48 (green), cCD58 (red), and rCD2 (blue), superimposed on domain 2 of each molecule. The first residue of domain 2 in each molecule (Glu-104 in cCD48, Glu-94 in cCD58, and Glu-99 in rCD2) is marked with a green sphere. B, the inter-domain contact region is shown enlarged for cCD48 and cCD58 with key non-linker interface residues drawn as ball and stick models. rCD2 is not shown because its interactions are similar to those of cCD58. The hydrogen bonds between the two IgSF domains of cCD48 are marked as dark blue dashed lines.

and 5 glycerol molecules that are ordered in the crystal and form hydrogen bonds with cCD48.

The overall structure of cCD48 is very similar to that of rat CD2 (24) and cCD58 (Fig. 1A) (27). The rat CD2 C2-set IgSF domains of all three proteins are not significantly different (r.m.s.d. values of 0.4 and 0.5 Å for superposition of 77 equivalent α atoms, respectively). Comparison of the inter-domain angles in these molecules shows that the ligand-binding domain of cCD48 is slightly more upright than that of cCD58 (by $\sim 3^\circ$), which is in turn slightly more upright than CD2 (by $\sim 5^\circ$; Fig. 1A). Two hydrophobic interactions fix the inter-domain angle in both srCD2 and cCD58 (Fig. 1B). In cCD48, one of these interactions is conserved (between Ile-12 and Val-168), and the other is replaced by a weaker hydrogen bond involving

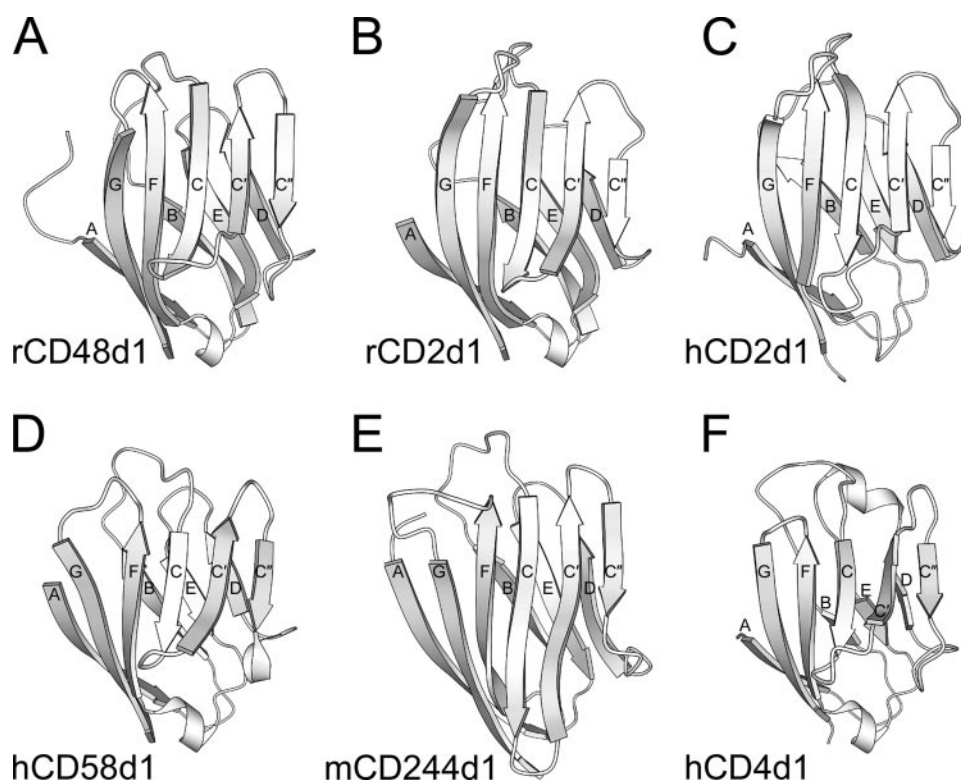


FIGURE 2. **Comparison of V-set IgSF domain folds.** Illustrations of the secondary structure of the membrane distal domains of rCD48 (A), rCD2 (B), hCD2 (C), hCD58 (D), mCD244 (E), and hCD4 (F) are shown in the same orientation, as defined by superposition of each domain onto that of rCD48. The β -strands of each domain are labeled according to the convention for IgSF domains.

TABLE 2

Binding data for mutants of CD48

Binding was assayed by surface plasmon resonance. Chimeras consisting of the extracellular region of rCD48, containing the indicated mutations, and domains 3 and 4 of rat CD4, were immobilized via the OX68 antibody or via biotinylation and binding to streptavidin. Binding to the OX45 antibody and to a high avidity (dimeric) form of the rCD2 ligand-binding domain joined to GST (CD2d1-GST) are indicated as follows: ++, WT binding; +, reduced binding; –, no binding. Dissociation constants (K_d) were calculated for the binding of srCD2 to mutants by equilibrium analysis. ND indicates a measurement was not determined.

| CD48 mutation | OX45 | CD2d1-GST | rCD2 K_d |
|---------------|-----------------|-----------|--------------------|
| | | | μM |
| WT | ++ | ++ | 37 |
| Q30K | ND ^a | ND | 34 |
| R31A | – | + | 168 |
| R31K | ++ | + | 108 |
| R31Y | – | + | 22 |
| T33A | ++ | + | 42 |
| L35A | ND | ND | >1500 ^b |
| H36A | ++ | ++ | 54 |
| Q40A | ND | ND | 294 |
| Q40R | ND | ND | 439 |
| K41A | ++ | – | ND |
| K41D | ++ | – | ND |
| K41Y | ++ | – | ND |
| E44A | ++ | + | >1500 ^b |
| E44D | ++ | + | 102 |
| E44Q | ++ | + | 50 |
| E44R | ++ | – | ND |
| E44Y | ++ | – | ND |
| F54A | ++ | – | ND |
| E55R | ND | ND | 17 |
| R87A | ND | ND | >1500 ^b |
| L89A | ++ | + | >1500 ^b |
| T92A | ND | ND | 11 |
| E93A | – | + | >1500 ^b |

^a ND, not determined.

^b Binding was undetectable on injection of rCD2d1 at 1500 μM , therefore the K_d must be greater than this value.

Asn-10 and Arg-167. A salt bridge (between Lys-78 and Glu-104) is present on the other side of the linker, straightening the molecule slightly (Fig. 1B). Arg-167 is replaced by proline in WT CD48, so the hydrogen bond with Asn-10 cannot form in the native protein. The other interactions are likely to occur, however, as Glu-104 is replaced with an aspartic acid in WT CD48, and Val-168 is present in both cCD48 and WT CD48. Overall, WT rCD48 can be expected to have the same topology as the chimera and CD2, with the ligand binding surface lying close to the top of the molecule. As in the case of cCD58 (27), cCD48 does not form the distinctive lattice contacts involving the ligand binding GFCC'C" face seen in crystals of both rat (24) and human (25) CD2, due perhaps to the high net charges of the central regions of the equivalent surfaces of CD48 (positive) and CD58 (negative (27)).

Structure of the CD48 Ligand-binding Domain—The rat CD48

ligand-binding domain has the expected IgSF V-set AGF-CC'C":DEB topology. It is grossly similar to the corresponding domains of CD2 and CD58 (Fig. 2, r.m.s.d. values of 1.18, 1.17, and 1.19 Å for 86, 85, and 82 equivalent C α atoms for rat CD2, human CD2 and CD58, respectively) but less similar to the equivalent domain of mouse CD244 (Fig. 2, r.m.s.d. of 1.65 Å for 83 equivalent C α atoms). As in the case of the other CD2 subset IgSF proteins, CD48 lacks a canonical disulfide bond and the twist in the ligand-binding GFCC'C" β -sheet that is characteristic of, e.g., antibody variable domains. The strand orientations in CD48 also resemble those in CD244, CD2, and CD58, including the distinctive position of the C" β -strand and the short DE loop. However, differences also exist, reflecting the considerable divergence within the family as judged by their low sequence homology (e.g. 31% identity for rat CD48 and CD2); the FG loop is shorter in CD48 than in CD2 or CD58 (by 1 and 2 residues, respectively), and the CC' loop is longer (by 4 residues compared with CD2 and 3 residues compared with CD58). The real outlier within the subset is CD244, although this may be due in part to the different method of structure determination, i.e. NMR. CD244 has very long FG and CC' loops, and hydrogen bonding between the A and G strands that extends for the full length of the G strand, rather than for the C-terminal-most third or half of the strand only. Automated structure comparisons using DALI (51) selected CD4 (1cdy) as the most CD48-like structure in the Protein Data Bank (PDB), followed by CD2 (1qa9), CD58 (1ccz), and CD80 (1dr9). CD244 was only the 25th-most similar structure. Inspection of a superposition of the ligand-binding domains of CD48 and

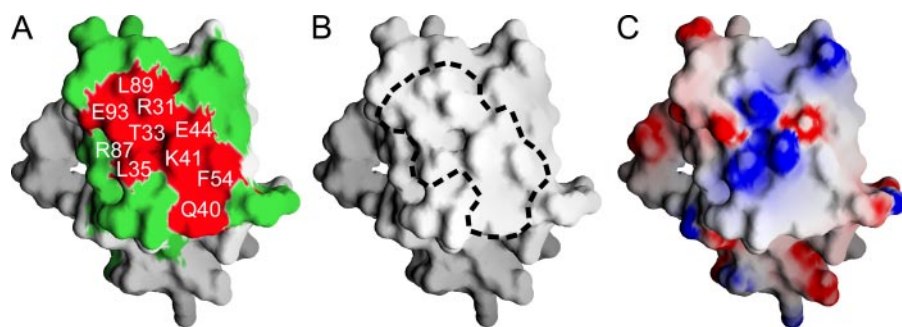


FIGURE 3. **The ligand binding face of rat CD48.** The surface of the V-set domain of rCD48 is shown oriented to reveal the ligand-binding GFCC'C'' face of the protein, as in Fig. 2. A, the surfaces of residues whose mutation disrupts CD2 binding are colored *red* and labeled, whereas those whose mutation has no effect are colored *green*. B, the surface is uncolored to reveal its flatness; the outline of the CD2 binding surface (as seen in A) is shown. C, the surface is colored by its native electrostatic potential calculated at neutral pH; *blue* represents positive potential, *white* represents neutral, and *red* represents negative potential contoured at ± 8.5 kT.

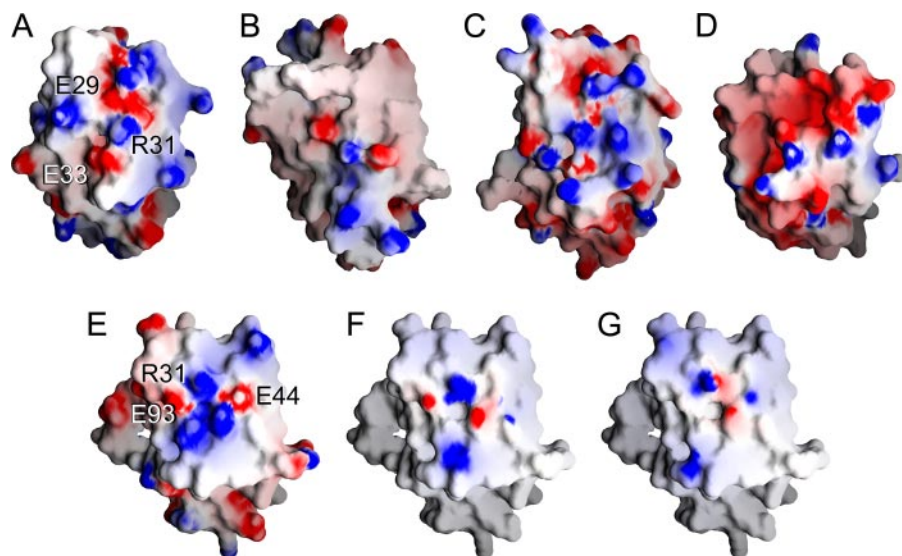


FIGURE 4. **The electrostatic potential of CD48-related proteins.** A–E, the surfaces of domain 1 from rCD2 (A), mCD244 (B), hCD2 (C), hCD58 (D) and, for comparison, rCD48 (E) are shown oriented as in Fig. 3, colored by the native electrostatic potential of the surface calculated at neutral pH; *blue* represents positive potential, *white* represents neutral, and *red* represents negative potential contoured at ± 8.5 kT. Residues referred to in the text are labeled. F and G, the electrostatic potential of rCD2 is shown projected onto the surface of rCD48 and contoured at ± 2.5 kT, when docked onto rCD48 by either simple superposition of the molecules onto the structure of the hCD58-hCD2 complex (F) or according to the improved model described in the text (G). It is clear that in the direct superposition model (F), regions of positive potential on CD2 align with regions of positive potential on the native CD48 surface (E) and a similar clash occurs in two regions of negative potential, likely resulting in electrostatic repulsion. These clashes are alleviated in the improved model (G).

CD4 revealed that the automatic procedure detects largely fortuitous similarities in the conformations adopted by loops of similar length (data not shown).

Ligand Binding Face of CD48—Residues whose “drastic” mutation was previously shown to disrupt CD2 binding (33) are all located in the ligand binding GFCC'C'' face of CD48. Additional drastic and alanine mutants were made to complete the analysis of the CD2 binding face. Representative surface plasmon resonance binding data for some of these mutants are shown in supplemental Fig. S3; the results for all mutants are summarized in Table 2. *In toto*, the drastic mutations delineate a contiguous surface consisting of three hydrophobic, two polar, and five charged residues (Fig. 3A). This surface is remarkably flat (Fig. 3B), as is that of rat CD2, and both are substantially flatter than the equivalent surfaces of the human proteins (Fig. 4). The average distance of surface atoms on the

GFCC'C'' face from the least-squares plane they form is 1.5 and 1.8 Å for rat CD48 and CD2, compared with 2.4 and 3.0 Å for human CD58 and CD2. The surface of mCD244 is the least flat of all the available structures: the r.m.s.d. of the surface atoms from a plane is 3.7 Å if all atoms are included, and 3.0 Å even if the atoms in the FG and CC' loops, which vary in conformation in the NMR structure, are removed. The CD48 ligand-binding surface is also highly charged (Fig. 3C), as in the case of its murine ligands, CD2 (Fig. 4A) (24) and CD244 (for which only the mouse structure is known, Fig. 4B) (16), but not to the extent of that of human CD2 (Fig. 4C) (25) and CD58 (Fig. 4D) (27).

Binding is perturbed by alanine substitutions of almost all the residues whose drastic mutation completely abrogates binding (Table 2). The exception is Thr-33, which is situated at the base of a pocket in the CD48 surface. This is in marked contrast to rat CD2 for which 4 of the 7 charged residues in the binding face can be mutated to alanine without substantially affecting binding affinity (Table 3) (26).

The CD48-CD2 Interaction—An initial model of the rat CD2-CD48 interaction can be based on superposition of CD2 and CD48 with their counterparts in the human CD2-CD58 complex (29). However, projection of the electrostatic potential of CD2 (Fig. 4A) onto CD48 in this arrangement (Fig. 4F) gives a substantial electrostatic

clash centered on Arg-31, Glu-44, and Glu-93 of CD48 and Arg-31, Glu-29, and Glu-33 of CD2. In addition, residue pairs expected to form salt bridges (*i.e.* CD2 Lys-43 with CD48 Glu-44, and CD2 Glu-41 with CD48 Arg-31 (33)) are not sufficiently close to allow the formation of such contacts. Finally, the model imposes steric clashes in the regions of the FG loops of CD2 and CD48. A second model (Fig. 5A) that differs by a $\sim 7^\circ$ rotation of CD48 about an axis perpendicular to the binding face and a ~ 3 Å translation toward the base of its GFCC'C'' face, and incorporates a degree of side-chain movement, alleviates the steric and electrostatic clashes (Fig. 4G) and allows the salt bridges to form (Fig. 5B). The new model also positions two additional pairs of charged side chains within range of interaction (*i.e.* CD48 Lys-41 and Glu-93 with CD2 Glu-29 and Arg-31, respectively, Fig. 5B), aligns the only hydrophobic residues on the interacting surfaces (*i.e.* CD48 L89 and CD2 L38, Fig. 5B), and

TABLE 3

Comparison of rCD2/rCD48 mutational data with the structural model

| Residue | Ala mutant binding | Other mutation(s) | Binding | Possible structural explanation |
|--|--------------------|---|---------------|--|
| rCD2 mutants (binding to rCD48) | | | | |
| His-12 ^a | ND ^b | Asp | ++ | Far from binding face |
| Asn-17 ^a | ND | Asp | ++ | Far from binding face |
| Asp-26 ^a | ND | Lys | ++ | Far from binding face |
| Asp-28 ^a | — | Lys | — | No contact with CD48; possibly stabilizing Lys-43 and Lys-45 on CD2 |
| Glu-29 ^a | — | Arg | — | Salt bridges to CD48 Arg-31 and Lys-41 |
| Arg-31 ^a | — | Tyr | — | Salt bridge to CD48 Glu-93 |
| Glu-33 ^a | ++ | Arg | — | Unclear; possible H-bond with CD48 Glu-93 |
| Arg-34 ^a | ++ | Asp | +++ | Far from binding face |
| Ser-36 ^a | ND | Glu | ++ | Edge of binding face, no contact with CD48 |
| Thr-37 ^a | ND | Lys | ++ | Edge of binding face, pointing away from CD48 |
| Leu-38 ^a | — | Tyr | — | Hydrophobic packing with CD48, especially Leu-89 |
| Glu-41 ^a | ++ | Arg | — | Salt bridge with CD48 Arg-31 ^c |
| Lys-43 ^a | + | Glu | — | Salt bridge with CD48 Glu-44 ^c |
| Lys-45 ^a | ND | Glu | ++ | Edge of binding face, no contact with CD48 |
| Met-46 ^a | ND | Tyr | ++ | Edge of binding face, no contact with CD48 |
| Lys-47 ^a | ND | Asp | ++ | Far from binding face |
| Phe-49 ^a | — | Arg | — | Hydrophobic packing with CD48, especially Leu-89 |
| Lys-51 ^a | ++ | Glu | + | Edge of binding face, may interact with CD48 Glu-91 |
| Ser-52 ^a | ND | Glu | + | Far from binding face |
| Glu-56 ^a | ++ | Arg | ++ | Far from binding face |
| Arg-70 ^a | ND | Glu | ++ | Far from binding face |
| Thr-79 ^a | ND | Glu | + | On binding face, but set back from CD48; space for larger side chain |
| Tyr-81 ^a | — | Ser | — | H-bond with Arg-87 |
| Thr-83 ^a | ND | Asp | + | Edge of binding face, pointing away from CD48 |
| Thr-86 ^a | ++ | Asp | — | Possible H-bond with CD48 Gln-40 |
| Arg-87 ^a | +++ | Glu | — | Very close to CD48, possible steric interference; may H-bond to Thr-38 |
| Asn-90 ^a | ND | Lys | + | Edge of binding face, no contact with CD48 |
| Asp-94 ^a | ND | Lys | ++ | Far from binding face |
| rCD48 mutants (binding to rCD2) | | | | |
| Lys-23 | ND | Glu ^c | ++ | Far from binding face |
| Ser-28 | ND | Glu ^c | ++ | Far from binding face |
| Gln-30 | ND | Lys | ++ | Edge of binding face, no contact with CD2 |
| Arg-31 | + ^a | Glu ^{a,c} , Lys Tyr ^a | + | Salt bridges with Glu-41 ^c and Glu-29 |
| Thr-33 | + | Arg ^c , Glu ^c | — | At base of pocket at centre of binding face (see Fig. 3), no contact with CD2, but no space for large side chain |
| Leu-35 | — | Arg ^c | — | No contact with CD2 but Arg would disrupt CD48 Arg-87 and Lys-41 |
| His-36 | + | Glu ^c | + | Internally pointing residue |
| Thr-38 | ND | Arg ^c | ++ | Possible H-bond with CD2 Arg-87, very close to CD2 FG loop |
| Asn-39 | ND | Asp ^c | ++ | Edge of binding face, pointing away from CD2 |
| Gln-40 | — | Arg | — | Possible H-bond with CD2 Thr-86 |
| Lys-41 | — | Glu ^c , Arg ^c , Asp, Tyr | — | Salt bridge with CD2 Glu-29 |
| Glu-44 | — ^a | Lys ^{a,b} , Arg ^a , Tyr ^a Asp ^a , Gln ^a | — + | Salt bridge with CD2 Lys-43 ^d |
| Phe-46 | ND | Asp ^c | ++ | Edge of binding face, no contact with CD2 |
| Lys-50 | ND | Glu ^c | ++ | Edge of binding face, no contact with CD2 |
| Thr-52 | ND | Arg ^c | ++ | Edge of binding face, no contact with CD2 |
| Phe-54 | — | Asp ^c | — | Unclear, see text |
| Glu-55 | ND | Arg | ++ | Edge of binding face, pointing away from CD2 |
| Lys-59 | ND | Glu ^c | ++ | Far from binding face |
| Tyr-85 | ND | Asp ^c | ++ | Far from binding face |
| Arg-87 | — | Glu ^c Asp ^c | — — | H-bond with CD2 Tyr-81 |
| Leu-89 | — | None | — | Hydrophobic packing with CD2, especially Leu-38 and Phe-49 |
| His-90 | ND | Asp ^c | ++ | Internally pointing residue |
| Glu-91 | ND | Lys ^c | ++ | Edge of binding face, may interact with CD2 Lys-51 |
| Thr-92 | ++ | Arg | Not expressed | Edge of binding face, no contact with CD2 |
| Glu-93 | — | Arg ^c Asp ^c | — ++ | Salt bridge to CD2 Arg-31; possible H-bond to CD2 Glu-33 |
| Gln-95 | ND | Arg ^c | ++ | Edge of binding face, no contact with CD2 |
| Glu-101 | ND | Arg ^c | ++ | Far from binding face |

^a From Ref. 26.^b ND, not determined.^c From Ref. 33.^d Interaction known from charge swap mutagenesis (33).

accounts for virtually all the CD48 and CD2 mutational data (Table 3). The only exception is Phe-54 of CD48, which is not involved in any contacts but whose mutation to Ala disrupts CD2 binding. This residue may influence binding indirectly by stabilizing the aliphatic region of the side chain of Lys-41 of CD48 via a hydrophobic interaction, perhaps in conjunction with Tyr-81 of CD2 in the complex. Clear differences in charge distribution (Fig. 4, A and B) and FG and CC' loop conforma-

tion (Fig. 2) between rat CD2 and mouse CD244 (16), suggest that the CD244-CD48 interaction may involve substantially different contacts.

Thermodynamics of the Rat CD48-CD2 Interaction—The flat binding surfaces of CD2 and CD48 would be expected to form an interface exhibiting greater surface complementarity than for the CD2-CD58 complex, and, visually, this appears to be the case (Fig. 5C). This ought to confer a higher affinity on the

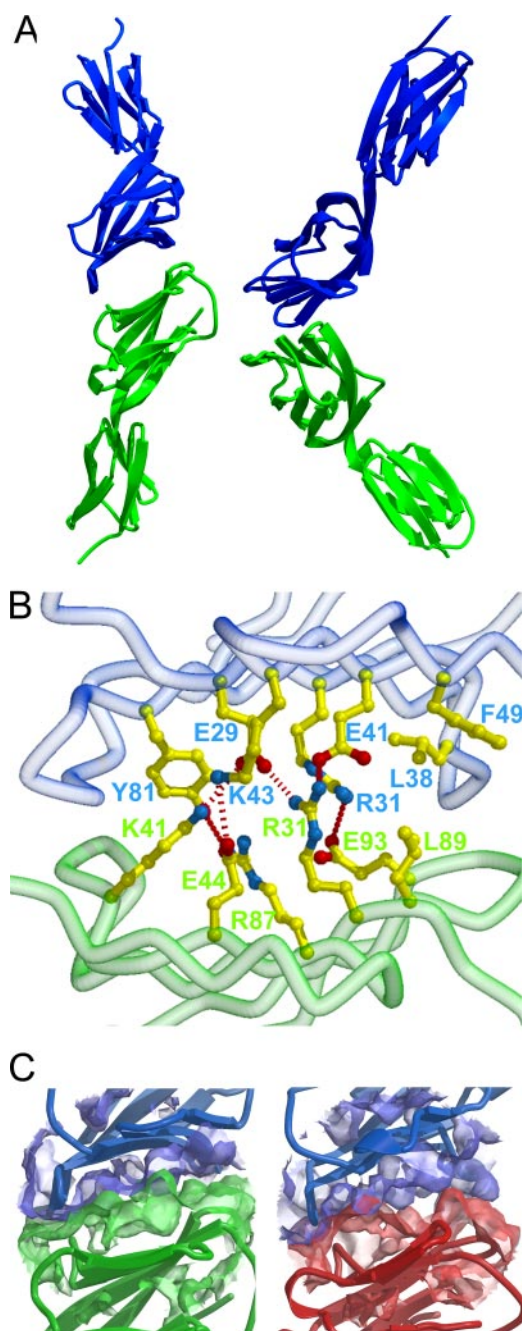


FIGURE 5. Modeling the rCD48-rCD2 complex. A, two orthogonal views of a ribbon representation of the likely complex formed between the full extracellular domains of rat CD2 (blue) and rat CD48 (green, modeled on cCD48). B, expanded view of the interface, with the side chains of the residues most likely to be involved in the interaction shown as ball-and-stick representations. Hydrogen bonds are shown as dashed red lines. C, comparison of the modeled rat CD2-CD48 complex (left) with the solved human CD2-CD58 complex (right, CD58 in red). The solvent-accessible molecular surface of the separate proteins is shown semi-transparently over a representation of their secondary structure to illustrate the complementarity of the binding surfaces.

interaction, but the interaction of the rat proteins is in fact 4-fold weaker than that of the human proteins (17, 52), implying that the detail of the interactions of the human and rat proteins is substantially different. In the absence of a complex structure, the thermodynamics of CD2-CD48 binding were investigated.

In a preliminary analysis, the equilibrium affinity of srCD2 for an immobilized WT CD48-CD4 chimera was determined using surface plasmon resonance at several temperatures. van't Hoff analysis of the data (Fig. 6A and Table 4) indicated that the interaction is driven by similarly small, favorable enthalpic and entropic components ($\sim 2\text{--}4$ kcal mol $^{-1}$ at 25 °C). Precise measurement of the thermodynamic properties of the interaction was carried out using isothermal calorimetry (Fig. 6B and Table 5). The affinity calculated for the interaction of rCD48 with the CD48-binding domain of rat CD2 (CD2d1 (32), $K_a = 5.5 \times 10^4$ M $^{-1}$ at 25 °C) using isothermal titration calorimetry is in good agreement with that obtained by surface plasmon resonance ($K_a = 3.2 \times 10^4$ M $^{-1}$ (52)). The measured enthalpy is indeed small, and temperature-dependent ($\Delta H_{\text{obs}} = -3.5$ kcal mol $^{-1}$ at 25 °C), and the entropic term is also small and favorable ($T\Delta S = 3.6$ kcal mol $^{-1}$ at 25 °C, Table 5). Increasing the ionic strength did not significantly affect the binding constant: a slight reduction in the enthalpy term was balanced by a slight increase in entropy (Table 5). Overall, the data indicate that the net contribution of electrostatic interactions to binding is very limited, as noted previously (26).

The slope of the plot of ΔH_{obs} against temperature (Fig. 6C) was used to estimate the change in heat capacity (ΔC_p) on binding, which is generally thought to be the product of solvent-mediated effects and as such can be used to analyze the contribution of the "hydrophobic effect" to binding. The model of the CD2-CD48 complex predicts that the surface area buried by the interaction is ~ 1250 Å 2 (defined as the area inaccessible to a spherical probe of radius 1.4 Å; the value for the CD2-CD58 complex is 1320 Å 2). Assuming a ratio of non-polar to polar buried surface of 58%, the average of many such interactions (Ref. 53, the value for the CD2-CD58 complex is 56.8%), the predicted ΔC_p for this interaction would be -160 cal mol $^{-1}$ K $^{-1}$. The value calculated from the isothermal titration calorimetry data was -180 cal mol $^{-1}$ K $^{-1}$ (Table 5), in good agreement with the theoretical value for the modeled complex.

Thermodynamics of CD48 Binding by Rat CD2 Mutated at Arg-87—Mutating Arg-87 of rat CD2 to alanine has been shown previously to increase the binding affinity by ~ 5 -fold (26). The modeled interaction of CD2 and CD48 is constrained by a steric clash in the region of Arg-87, *i.e.* the CD2 FG loop, suggesting that the loop limits the shape complementarity of the binding interface. Titration of srCD48 against CD2d1 mutated to alanine at position 87 confirmed the scale of the affinity increase resulting from the mutation ($K_a = 3.6 \times 10^5$ M $^{-1}$ at 25 °C; a 6- to 7-fold increase). The enhanced affinity has both enthalpic and entropic components: the ΔH is 450 cal mol $^{-1}$ more favorable, and the $T\Delta S$ is increased by 650 cal mol $^{-1}$ (Table 5). In contrast to WT CD2, changing the ionic strength of the solution results in considerably weaker binding of the R87A mutant to CD48 (Table 5) due to a reduction in the favorable entropy, with no compensating effect on enthalpy.

DISCUSSION

The mechanisms of weak, specific recognition at cell surfaces are perhaps best understood for interactions involving CD2 (reviewed in Ref. 20). The structures of unliganded human and rat CD2 and CD58, along with that of the complex of human CD2 and

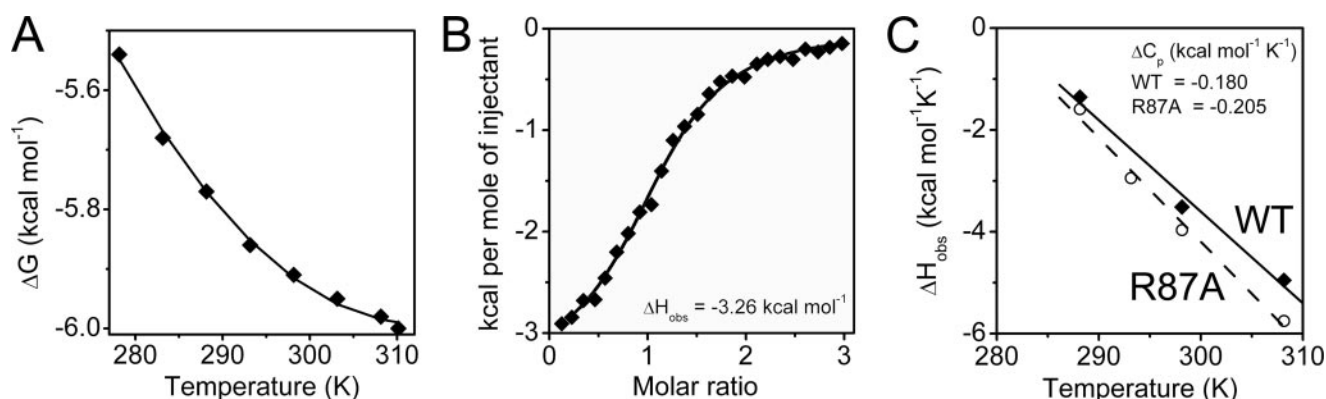


FIGURE 6. **Thermodynamics of the rCD2-rCD48 interaction.** A, van't Hoff plot of equilibrium binding affinity data for the rCD2-rCD48 interaction collected using surface plasmon resonance-based methodology at several temperatures. Non-linear curve fitting of the data (see "Experimental Procedures") yields estimates of the change in enthalpy (ΔH_{vH}) and entropy (ΔS_{vH}) on binding at an arbitrary temperature (T_0) and the change in heat capacity on binding ($\Delta C_{p,vH}$), which is assumed to be invariant with temperature. The data shown were fitted using two values of T_0 , namely 298.15 K (25 °C) and 310.15 K (37 °C), and the resulting curves superimpose. The estimates of ΔH_{vH} , ΔS_{vH} , and $\Delta C_{p,vH}$ from these fittings were -3666 cal mol⁻¹, 5.1 cal mol⁻¹ K⁻¹ and -214 cal mol⁻¹ K⁻¹ at 25 °C and -5432 cal mol⁻¹, 1.8 cal mol⁻¹ K⁻¹, and -225 cal mol⁻¹ K⁻¹ at 37 °C. Replicate experiments yielded the values given in Table 4. B, an example titration of rCD48 (2.35 mM) into an isothermal calorimetry cell containing rCD2 (0.128 mM) at pH 7.4 and 25 °C in a buffer containing 150 mM NaCl, fitted with a one-site binding model. Similar titrations were undertaken at various temperatures and a second ionic strength (500 mM NaCl), the results of which are summarized in Table 5. C, plot of observed enthalpy versus temperature for the interaction of rCD48 with WT rCD2d1 (◆) or R87A rCD2d1 (○). The slope of this plot gives the change in heat capacity (ΔC_p) on binding, the values of which are -180 cal mol⁻¹ K⁻¹ and -204 cal mol⁻¹ K⁻¹ for the interaction with WT and R87A rCD2d1, respectively.

CD58 highlighted the importance of charged contacts and poor surface complementarity (27, 29). The interaction of rat CD48 with CD2, characterized in detail here, differs from that of human CD2 and CD58 in that it is somewhat weaker, *i.e.* 4- to 5-fold, and part of a broader network of interactions, *i.e.* involving CD244 (2B4) and 2B4R, which CD48 also binds more strongly (3- to 4-fold).

The compatibility of rat CD2 domain 2 with the ligand-binding domains of CD58 (27, 31) and now, CD48, and the conservation of the inter-domain linker region sequences in all three proteins are consistent with early suggestions that this region has an important function, *i.e.* presentation of the ligand binding surface at the "top" of the molecule, facilitating ligand binding (24, 25, 27). Recent support for this idea has come from comparisons of CD48 and B7-1 as adhesive ligands in model lipid bi-layers (54). B7-1 and CD48 are likely to have similar overall dimensions, but the reduced tilt of domain 1 relative to domain 2 positions the plane of the ligand binding AGFCC'C" face of B7-1 parallel with the long axis of the molecule, rather than, as in the case of CD48 and CD2, almost orthogonal with it, necessitating "side-to-side" rather than "head-to-head" contacts with their ligands. The solution affinity of B7-1 for CD28 is ~30-fold higher than that of the CD48-CD2 interaction, and yet B7-1 inserted into model lipid bilayers is incapable of ligating CD28 on T cells unless CD48 is also present in the model bilayer (54). The simplest explanation for this is that the membranes need to be proximal before CD28 and B7-1 can interact. The observation that the positioning of the ligand-binding domain relative to the rest of the molecule has such an apparently large bearing on binding suggests that proteins at the cell surface are constrained vertically at the membrane, otherwise pivoting about the stalk region would be expected to overcome such constraints. Currently, there is much interest in the possibility that the functions of signaling proteins, such as phosphatases, are influenced by their dimensions orthogonal to the membrane (55). Such effects are likely to require that the vertical positions of such molecules are constrained. Our observations also suggest that

topological effects may contribute to the specificity of recognition at the cell surface.

The structure of the CD48 ligand-binding domain is the fourth such domain from the CD2 subset of the IgSF to be solved (*i.e.* along with CD2, CD58, and CD244), and the second from within the so-called SLAM subgrouping (56, 57). These domains share very limited sequence homology, and the CD48 structure is no more similar to CD2 or CD58 than CD2 is similar to CD58. Structurally, CD48 shares fewest similarities with CD244, even though both proteins clearly arose via duplications and remain closely linked. This suggests that the CD2 subset of the IgSF consists of very ancient proteins, and that further subdivisions of these proteins on structural grounds into, *e.g.* SLAM- and non SLAM-related groupings, is at best arbitrary.

Genomic analysis indicates that the *cd58* gene has been lost from the mouse genome, because, in addition to humans, *CD58* genes are present in zebrafish (accession number XM_694417), chickens (accession number CD215002), and mallard ducks (accession number AY032731). This implies that murine CD2 has gained specificity for CD48, which may have previously only bound the higher affinity ligand, CD244, possibly explaining why the CD2-CD48 interaction is weaker. Human CD2 binds CD48 but so weakly that the interaction is unlikely to be functional (58). An interesting question is: what features of CD48 allow it to bind multiple ligands? An explanation suggested by the new structural data is that the relatively flat binding surface of CD48 and limited number of charged residues compared with, *e.g.* CD58, allow CD48 to be unusually tolerant of variation in the binding surfaces of potential ligands. Clear evidence of this comes from the observation that, in addition to binding CD2, rat CD48 binds the orthologue of CD244 (rat 2B4 (15)) and a third ligand, 2B4R (14). 2B4 and 2B4R are closely related proteins that bind with comparable affinity to CD48.⁹

⁹ E. J. Evans and S. J. Davis, unpublished data.

Interestingly, however, most (*i.e.* 15 of 17) of the amino acids that distinguish these proteins align with residues forming the CD48-binding, GFCC'C" face of rat CD2.

Our most important findings concern the nature of the low affinity interaction of CD48 with CD2. We propose a model of the complex, which, although broadly similar, differs in detail from another based on simple superpositions of rat CD2 and CD48 with their counterparts in the human CD2-CD58 complex (29). We suggest that the new model is credible for the following reasons: 1) it avoids an electrostatic clash at the center of each binding surface and steric interference involving the FG loops of both proteins; 2) two residue pairs expected to form salt bridges according to charge-swap mutagenesis are brought into close proximity; 3) it positions two additional pairs of charged side chains, and a hydrophobic residue on each surface, within range of interaction; and 4) it accounts for virtually all the mutational data. The new model requires a 7° rotation and ~3-Å translation of CD48 relative to the position of CD58. If correct, it reveals considerable plasticity in the topology of ligand recognition by CD2.

The thermodynamic analysis provides further evidence that the ligand binding mechanisms of human and rat CD2 are substantially different. Whereas the rat interaction has roughly equivalent enthalpic and entropic components, a relatively high enthalpy overcomes a large entropic barrier for the interaction of human CD2 with CD58.⁷ The unfavorable entropy of the interaction of the human proteins likely results from restraining the somewhat flexible binding faces of human CD2 and CD58 in the complex (59) and from the ordering of solvent molecules between the poorly matched binding surfaces. It is conceivable that the unliganded rat proteins are much less con-

formationally flexible. The small enthalpic contribution to binding in the rat system suggests that the flat binding surfaces do not substantially increase van der Waals contacts between the proteins, because the enthalpy of binding (−3.5 kcal/mol) is approximately one-quarter of that of the human interaction (−12 kcal/mol) and one-third to one-sixth that measured for four antibody-protein antigen complexes interacting over comparable surface areas (60). Our model of the rat CD2-CD48 interaction also suggests that comparable numbers of hydrogen bonds and salt bridges form in the rat and human complexes (3 hydrogen bonds and 6–8 salt bridges *versus* 3 hydrogen bonds and 10 salt bridges, respectively (29)) and that both complexes lack large hydrophobic contacts. It is therefore unclear why the enthalpies of the human and rat interactions are so different. One possibility is that the unusual, interdigitating network of salt bridges seen in the complex of human CD2 and CD58, which may reduce unfavorable electrostatic interactions between similarly charged residues in the unliganded proteins (29), is likely to be absent from the rat CD2-CD48 interface. Analysis of the R87A mutant of rat CD2, for which binding to CD48 has a higher enthalpy, suggests that steric effects may also constrain the enthalpy of binding by preventing the close apposition of the two relatively flat binding surfaces over their entire area, although these effects are small ($\Delta\Delta H \leq 0.5$ kcal/mol). An explanation for the enhanced binding entropy of the mutant and its ionic strength dependence is that the better fit of the two surfaces leads to the formation of additional charge-charge interactions, resulting in the release of previously bound ions to the solvent.

The clear differences in the human and rat CD2-ligand interactions, despite the obvious relatedness of these two molecules, fits an emerging view that the binding properties of cell surface molecules are very heterogeneous. Structures of the complexes formed between CD152 (CTLA-4) and its ligands CD80 (61) and CD86 (62), for example, reveal that, in contrast to the interactions of CD2, binding involves a very high degree of surface complementarity and that there are many fewer electrostatic contacts. Binding in these instances is weak, because the proteins interact over a relatively small area and the reaction is constrained, as in the case of the human CD2-CD58 interac-

TABLE 4

Non-linear van't Hoff analysis of SPR data for the binding of WT rCD2d1 to WT rCD48-CD4 chimera

| T_0^a | ΔH_{vH} | $T\Delta S_{\text{vH}}$ | $\Delta C_{\text{p,vH}}$ |
|---------|------------------------|-------------------------|---------------------------------------|
| °C | cal mol ^{−1} | | cal mol ^{−1} K ^{−1} |
| 25 | −3500 ± 400 | 2000 ± 300 | −205 ± 13 |
| 37 | −5900 ± 400 | 200 ± 300 | −205 ± 13 |

^a T_0 is the arbitrary reference temperature used in fitting the van't Hoff equation, and therefore the temperature at which the given estimates of temperature dependent thermodynamic terms apply; see "Experimental Procedures."

TABLE 5

Summary of thermodynamic data for the binding of srCD48 to WT and R87A rCD2d1

srCD48 was titrated into an isothermal calorimetry cell containing either WT or R87A rCD2d1 at various temperatures and ionic strengths, and the resulting titration curves were fitted with a one-site binding model (Fig. 6B) to derive values for the stoichiometry, the association constant (K_a), and the change in enthalpy on binding (ΔH_{obs}). Other properties were calculated from these measurements.

| [NaCl] | Temp. | [rCD2d1] | Stoichiometry | K_a | K_d^a | ΔH_{obs} | ΔG_{calc}^b | $T\Delta S_{\text{calc}}^c$ |
|--------------------|-------|----------|---------------|-----------------------------------|---------|-------------------------|----------------------------|-----------------------------|
| mM | °C | μM | | M ^{−1} × 10 ⁵ | μM | | cal mol ^{−1} | |
| WT rCD2d1 | | | | | | | | |
| 150 | 15 | 92.7 | 0.93 ± 0.02 | 0.83 ± 0.10 | 12.0 | −1355 ± 41 | −6481 | 5346 |
| 150 | 25 | 107.7 | 1.10 ± 0.01 | 0.55 ± 0.02 | 18.2 | −3514 ± 43 | −6463 | 2949 |
| 150 | 35 | 93.8 | 1.05 ± .007 | 0.67 ± 0.03 | 14.9 | −4952 ± 52 | −6800 | 1848 |
| 500 | 25 | 103.1 | 1.02 ± 0.02 | 0.52 ± 0.05 | 19.2 | −2533 ± 76 | −6429 | 3896 |
| R87A rCD2d1 | | | | | | | | |
| 150 | 15 | 83.5 | 1.06 ± 0.01 | 3.70 ± 0.38 | 2.7 | −1592 ± 23 | −7342 | 5750 |
| 150 | 20 | 86.2 | 0.99 ± 0.01 | 3.77 ± 0.29 | 2.7 | −2947 ± 37 | −7480 | 4533 |
| 150 | 25 | 103.1 | 1.14 ± 0.002 | 3.62 ± 0.01 | 2.8 | −3966 ± 126 | −7584 | 3618 |
| 150 | 35 | 41.2 | 1.06 ± 0.01 | 2.79 ± 0.22 | 3.6 | −5752 ± 96 | −7679 | 1927 |
| 500 | 25 | 51.6 | 1.12 ± 0.01 | 2.18 ± 0.13 | 4.6 | −4034 ± 50 | −7283 | 3249 |

^a $K_d = 1/K_a$.

^b $\Delta G_{\text{calc}} = -RT \ln(K_a)$.

^c $T\Delta S_{\text{calc}} = \Delta H_{\text{obs}} - \Delta G_{\text{calc}}$.

tion, by a large, and as yet unexplained, entropic barrier.¹⁰ Entropic factors make even larger contributions to the weak affinities of TCRs for their peptide-major histocompatibility complex ligands (63). Much has been made of the significance of this for the TCR in terms of potential repertoire expansion or in the context of the function of the TCR as a molecule that scans extremely large numbers of potential ligands before undergoing conformational rearrangements allowing stable binding with cognate ligands (63, 64). As is now clear, the thermodynamics of TCR interactions are not that unusual and may simply reflect the fact that TCR ligands are cradled in intrinsically flexible loops at the "tops" of the variable domains. The use of these loops is in turn a direct consequence of the genetic mechanism generating diversity.

In conclusion, the binding face of rat CD48 appears to be ideally suited to binding multiple ligands while maintaining low affinity for each of them. It is conceivable that cross-reactive interactions of this type fuelled the initial expansion of CD2-related genes. For the human and rat CD2 homologues, however, it can probably be safely concluded that the major factor constraining their evolution is that their interactions should remain weak and specific.

Acknowledgments—We are grateful to the staff of beamlines BM14 and ID2 at the European Synchrotron Radiation Facility (Grenoble, France) for assistance with crystallographic data collection and R. Esnouf for assistance with angle calculations and figure preparation.

REFERENCES

- Engel, P., Eck, M. J., and Terhorst, C. (2003) *Nat. Rev. Immunol.* **3**, 813–821
- Sayos, J., Wu, C., Morra, M., Wang, N., Zhang, X., Allen, D., van Schaik, S., Notarangelo, L., Geha, R., Roncarolo, M. G., Oettgen, H., De Vries, J. E., Aversa, G., and Terhorst, C. (1998) *Nature* **395**, 462–469
- Kiel, M. J., Yilmaz, O. H., Iwashita, T., Terhorst, C., and Morrison, S. J. (2005) *Cell* **121**, 1109–1121
- Killeen, N., Stuart, S. G., and Littman, D. R. (1992) *EMBO J.* **11**, 4329–4336
- Teh, S. J., Killeen, N., Tarakhovsky, A., Littman, D. R., and Teh, H. S. (1997) *Blood* **89**, 1308–1318
- Bachmann, M. F., Barner, M., and Kopf, M. (1999) *J. Exp. Med.* **190**, 1383–1392
- van der Merwe, P. A. (1999) *J. Exp. Med.* **190**, 1371–1374
- Dumont, C., Deas, O., Hebib, C., Durrbach, A., Hirsch, F., Charpentier, B., and Senik, A. (2001) *Transplant Proc.* **33**, 199–200
- Gonzalez-Cabrero, J., Wise, C. J., Latchman, Y., Freeman, G. J., Sharpe, A. H., and Reiser, H. (1999) *Proc. Natl. Acad. Sci. U. S. A.* **96**, 1019–1023
- Brown, M. H., Boles, K., van der Merwe, P. A., Kumar, V., Mathew, P. A., and Barclay, A. N. (1998) *J. Exp. Med.* **188**, 2083–2090
- Garni-Wagner, B. A., Purohit, A., Mathew, P. A., Bennett, M., and Kumar, V. (1993) *J. Immunol.* **151**, 60–70
- Schuhmachers, G., Ariizumi, K., Mathew, P. A., Bennett, M., Kumar, V., and Takashima, A. (1995) *J. Invest. Dermatol.* **105**, 592–596
- Schuhmachers, G., Ariizumi, K., Mathew, P. A., Bennett, M., Kumar, V., and Takashima, A. (1995) *Eur. J. Immunol.* **25**, 1117–1120
- Kumaresan, P. R., Stepp, S. E., Bennett, M., Kumar, V., and Mathew, P. A. (2000) *Immunogenetics* **51**, 306–313
- Kumaresan, P. R., Stepp, S. E., Verrett, P. C., Chuang, S. S., Boles, K. S., Lai, W. C., Ryan, J. C., Bennett, M., Kumar, V., and Mathew, P. A. (2000) *Mol. Immunol.* **37**, 735–744
- Ames, J. B., Vyas, V., Lusin, J. D., and Mariuzza, R. (2005) *Biochemistry* **44**, 6416–6423
- van der Merwe, P. A., Barclay, A. N., Mason, D. W., Davies, E. A., Morgan, B. P., Tone, M., Krishnam, A. K., Ianelli, C., and Davis, S. J. (1994) *Biochemistry* **33**, 10149–10160
- van der Merwe, P. A., McPherson, D. C., Brown, M. H., Barclay, A. N., Cyster, J. G., Williams, A. F., and Davis, S. J. (1993) *Eur. J. Immunol.* **23**, 1373–1377
- Mavaddat, N., Mason, D. W., Atkinson, P. D., Evans, E. J., Gilbert, R. J., Stuart, D. I., Fennelly, J. A., Barclay, A. N., Davis, S. J., and Brown, M. H. (2000) *J. Biol. Chem.* **275**, 28100–28109
- Davis, S. J., Ikemizu, S., Wild, M. K., and van der Merwe, P. A. (1998) *Immunol. Rev.* **163**, 217–236
- van der Merwe, P. A., and Barclay, A. N. (1994) *Trends Biochem. Sci.* **19**, 354–358
- van der Merwe, P. A., and Davis, S. J. (2003) *Annu. Rev. Immunol.* **21**, 659–684
- Davis, S. J., Ikemizu, S., Evans, E. J., Fugger, L., Bakker, T. R., and van der Merwe, P. A. (2003) *Nat. Immunol.* **4**, 217–224
- Jones, E. Y., Davis, S. J., Williams, A. F., Harlos, K., and Stuart, D. I. (1992) *Nature* **360**, 232–239
- Bodian, D. L., Jones, E. Y., Harlos, K., Stuart, D. I., and Davis, S. J. (1994) *Structure* **2**, 755–766
- Davis, S. J., Davies, E. A., Tucknott, M. G., Jones, E. Y., and van der Merwe, P. A. (1998) *Proc. Natl. Acad. Sci. U. S. A.* **95**, 5490–5494
- Ikemizu, S., Sparks, L. M., van der Merwe, P. A., Harlos, K., Stuart, D. I., Jones, E. Y., and Davis, S. J. (1999) *Proc. Natl. Acad. Sci. U. S. A.* **96**, 4289–4294
- Sun, Z. Y., Dotsch, V., Kim, M., Li, J., Reinherz, E. L., and Wagner, G. (1999) *EMBO J.* **18**, 2941–2949
- Wang, J. H., Smolyar, A., Tan, K., Liu, J. H., Kim, M., Sun, Z. Y., Wagner, G., and Reinherz, E. L. (1999) *Cell* **97**, 791–803
- Jones, S., and Thornton, J. M. (1996) *Proc. Natl. Acad. Sci. U. S. A.* **93**, 13–20
- Butters, T. D., Sparks, L. M., Harlos, K., Ikemizu, S., Stuart, D. I., Jones, E. Y., and Davis, S. J. (1999) *Protein Sci.* **8**, 1696–1701
- Driscoll, P. C., Cyster, J. G., Campbell, I. D., and Williams, A. F. (1991) *Nature* **353**, 762–765
- van der Merwe, P. A., McNamee, P. N., Davies, E. A., Barclay, A. N., and Davis, S. J. (1995) *Curr. Biol.* **5**, 74–84
- Mizushima, S., and Nagata, S. (1990) *Nucleic Acids Res.* **18**, 5322
- Harlos, K. (1992) *J. Appl. Crystallogr.* **25**, 536–538
- Otwinowski, Z., and Minor, W. (1997) *Methods Enzymol.* **276**, 307–326
- Navaza, J. (1994) *Acta Crystallogr. Sect. A* **50**, 157–163
- Brunger, A. T., Adams, P. D., Clore, G. M., DeLano, W. L., Gros, P., Grosse-Kunstleve, R. W., Jiang, J. S., Kuszewski, J., Nilges, M., Pannu, N. S., Read, R. J., Rice, L. M., Simonson, T., and Warren, G. L. (1998) *Acta Crystallogr. Sect. D Biol. Crystallogr.* **54**, 905–921
- Cowan, K. D., and Main, P. (1996) *Acta Crystallogr. Sect. A* **52**, 43–48
- Jones, T. A., Zou, J. Y., Cowan, S. W., and Kjeldgaard, (1991) *Acta Crystallogr. A* **47**, 110–119
- Stuart, D. I., Levine, M., Muirhead, H., and Stammers, D. K. (1979) *J. Mol. Biol.* **134**, 109–142
- Esnouf, R. M. (1997) *J. Mol. Graph.* **15**, 133–138
- Merritt, E. A., and Murphy, M. E. P. (1994) *Acta Crystallogr. Sect. D Biol. Crystallogr.* **50**, 869–873
- Nicholls, A., Sharp, K. A., and Honig, B. (1991) *Proteins* **11**, 281–296
- Jackson, R. M., Gabb, H. A., and Sternberg, M. J. (1998) *J. Mol. Biol.* **276**, 265–285
- Wiseman, T., Williston, S., Brandts, J. F., and Lin, L. N. (1989) *Anal. Biochem.* **179**, 131–137
- Ladbury, J. E., and Chowdhry, B. Z. (1996) *Chem. Biol.* **3**, 791–801
- Yoo, S. H., and Lewis, M. S. (1995) *Biochemistry* **34**, 632–638
- Spolar, R. S., Livingstone, J. R., and Record, M. T., Jr. (1992) *Biochemistry* **31**, 3947–3955
- Davis, S. J., Puklavec, M. J., Ashford, D. A., Harlos, K., Jones, E. Y., Stuart, D. I., and Williams, A. F. (1993) *Protein Eng.* **6**, 229–232

¹⁰ A. V. Collins, D. W. Brodie, R. O'Brien, P. A. van der Merwe, S. J. Davis, and J. E. Ladbury, unpublished data.

51. Holm, L., and Sander, C. (1995) *Trends Biochem. Sci.* **20**, 478–480
52. van der Merwe, P. A., Brown, M. H., Davis, S. J., and Barclay, A. N. (1993) *EMBO J.* **12**, 4945–4954
53. Spolar, R. S., and Record, M. T., Jr. (1994) *Science* **263**, 777–784
54. Bromley, S. K., Iaboni, A., Davis, S. J., Whitty, A., Green, J. M., Shaw, A. S., Weiss, A., and Dustin, M. L. (2001) *Nat. Immunol.* **2**, 1159–1166
55. Choudhuri, K., Wiseman, D., Brown, M. H., Gould, K., and van der Merwe, P. A. (2005) *Nature* **436**, 578–582
56. Veillette, A., and Latour, S. (2003) *Curr. Opin. Immunol.* **15**, 277–285
57. Wang, N., Morra, M., Wu, C., Gullo, C., Howie, D., Coyle, T., Engel, P., and Terhorst, C. (2001) *Immunogenetics* **53**, 382–394
58. Arulanandam, A. R., Moingeon, P., Concino, M. F., Recny, M. A., Kato, K., Yagita, H., Koyasu, S., and Reinherz, E. L. (1993) *J. Exp. Med.* **177**, 1439–1450
59. Kitao, A., and Wagner, G. (2000) *Proc. Natl. Acad. Sci. U. S. A.* **97**, 2064–2068
60. Schwarz, F. P., Tello, D., Goldbaum, F. A., Mariuzza, R. A., and Poljak, R. J. (1995) *Eur. J. Biochem.* **228**, 388–394
61. Stamper, C. C., Zhang, Y., Tobin, J. F., Erbe, D. V., Ikemizu, S., Davis, S. J., Stahl, M. L., Seehra, J., Somers, W. S., and Mosyak, L. (2001) *Nature* **410**, 608–611
62. Schwartz, J. C., Zhang, X., Fedorov, A. A., Nathenson, S. G., and Almo, S. C. (2001) *Nature* **410**, 604–608
63. Willcox, B. E., Gao, G. F., Wyer, J. R., Ladbury, J. E., Bell, J. I., Jakobsen, B. K., and van der Merwe, P. A. (1999) *Immunity* **10**, 357–365
64. Wu, L. C., Tuot, D. S., Lyons, D. S., Garcia, K. C., and Davis, M. M. (2002) *Nature* **418**, 552–556

Crystal Structure and Binding Properties of the CD2 and CD244 (2B4)-binding Protein, CD48

Edward J. Evans, Mónica A. A. Castro, Ronan O'Brien, Alice Kearney, Heather Walsh, Lisa M. Sparks, Michael G. Tucknott, Elizabeth A. Davies, Alexandre M. Carmo, P. Anton van der Merwe, David I. Stuart, E. Yvonne Jones, John E. Ladbury, Shinji Ikemizu and Simon J. Davis

J. Biol. Chem. 2006, 281:29309-29320.

doi: 10.1074/jbc.M601314200 originally published online June 27, 2006

Access the most updated version of this article at doi: [10.1074/jbc.M601314200](https://doi.org/10.1074/jbc.M601314200)

Alerts:

- [When this article is cited](#)
- [When a correction for this article is posted](#)

[Click here](#) to choose from all of JBC's e-mail alerts

Supplemental material:

<http://www.jbc.org/content/suppl/2006/06/27/M601314200.DC1>

This article cites 64 references, 13 of which can be accessed free at

<http://www.jbc.org/content/281/39/29309.full.html#ref-list-1>